Electrochemistry of Carbidopentaruthenium C_{60} Complexes and Related Clusters

Audrey J. Babcock, Jinghong Li, Kwangyeol Lee, and John R. Shapley*

Department of Chemistry, University of Illinois, Urbana, Illinois 61801

Received July 11, 2002

The electrochemical behavior of the face-coordinated C_{60}-carbidopentaruthenium cluster complexes $Ru_5C(CO)_{11}(PPh_3)(\mu_3\text{-}\eta^2,\eta^2,\eta^2\text{-}C_{60})$ (**1**), $Ru_5C(CO)_{10}(\mu\text{-}\eta^1,\eta^1\text{-dppf})(\mu_3\text{-}\eta^2,\eta^2,\eta^2\text{-}C_{60})$ (**2**) (dppf = 1,1′-bis(diphenylphosphino)ferrocene), and $PtRu_5C(CO)_{11}(\eta^2\text{-dppe})(\mu_3\text{-}\eta^2,\eta^2,\eta^2\text{-}C_{60})$ (**3**) (dppe = 1,2-bis(diphenylphosphino)ethane) has been examined by cyclic voltammetry, rotating disk electrode voltammetry, and differential pulse voltammetry methods. The behavior of compounds $Ru_5C(CO)_{15}$ (**4**), $Ru_5C(CO)_{14}(PPh_3)$ (**5**), $Ru_5C(CO)_{13}(\mu\text{-}\eta^1,\eta^1\text{-dppf})$ (**6**), $PtRu_5C(CO)_{16}$ (**7**), and $PtRu_5C(CO)_{14}(\eta^2\text{-dppe})$ (**8**) was studied also for comparison. For both **1** and **3**, the voltammetric scans show an initial irreversible two-electron reduction feature, followed by three quasi-reversible, one-electron reductions of the C_{60} ligand. In contrast, similar scans for **2** indicate an initial quasi-reversible, one-electron reduction of the C_{60} ligand that is dynamically coupled with a second one-electron, irreversible reduction. Stepwise reduction of the C_{60} ligand proceeds at more negative potentials. Interpretation of the electrochemical behavior of compounds **1**−**8** has been enhanced by studying their chemical reduction with cobaltocene. In all cases uptake of two electrons results in irreversible loss of a CO ligand from the cluster, and the resulting dianionic complexes have been characterized by their IR (ν_{CO}) spectra.

Introduction

The capacity of C_{60} to undergo successive one-electron reductions is a hallmark of its physical properties. Depending on the solvent system, temperature, and scan rate employed, up to six reversible one-electron reductions of C_{60} can be observed.[1] Various organic derivatives of C_{60} have also been studied in order to observe the effect of derivatization on the fullerene electrochemical behavior.[2,3]

Metal complexes of C_{60} are of interest due to possible interplay between the redox properties of C_{60} and of the metal center. Studies of η^2-bonded C_{60} complexes have shown that the first two or three reductions of the C_{60} ligand still occur after derivatization[4,5] and that these reductions usually cause a decrease in stability of the metal−fullerene bond.[4] However, metal cluster complexes of C_{60} in the $\mu_3\text{-}\eta^2,\eta^2,\eta^2$ bonding mode are more robust,[6] and electrochemical studies of the face-bonded trimetallic complexes $Os_3(CO)_8(L)(\mu_3\text{-}\eta^2,\eta^2,\eta^2\text{-}C_{60})$ (L = CO, PMe_3)[7a] and $H_3Re_3(CO)_8(L)(\mu_3\text{-}\eta^2,\eta^2,\eta^2\text{-}C_{60})$ (L = CO, PPh_3)[7b] have demonstrated the occurrence of four successive reductions of the complexes without evidence of decomposition. Recently, a unique $Rh_6(\mu_3\text{-}\eta^2,\eta^2,\eta^2\text{-}C_{60})_2$ bis-fullerene cluster sandwich compound has been shown to accept up to six electrons (three for each C_{60} ligand) in a completely reversible fashion.[8]

The complexes $Ru_5C(CO)_{11}(PPh_3)(\mu_3\text{-}\eta^2,\eta^2,\eta^2\text{-}C_{60})$[6b,c] (**1**), $Ru_5C(CO)_{10}(\mu\text{-}\eta^1,\eta^1\text{-dppf})(\mu_3\text{-}\eta^2,\eta^2,\eta^2\text{-}C_{60})$[6c] (**2**), and $PtRu_5C(CO)_{11}(\eta^2\text{-dppe})(\mu_3\text{-}\eta^2,\eta^2,\eta^2\text{-}C_{60})$[6c] (**3**) represent an intriguing combination of an electroactive $\{Ru_5C\}$ metal core[9−12] with the fullerene ligand. Furthermore, $PtRu_5C(CO)_{16}$[13] has been used as a single-source molecular precursor for the formation of carbon-supported $[PtRu_5]$ nanoparticle electrocatalysts,[14−16] and the related de-

(1) (a) Dubois, D.; Kadish, K. M.; Flanagan, S.; Wilson, L. J. *J. Am. Chem. Soc.* **1991**, *113*, 7773. (b) Xie, Q.; Perez-Cordero, E.; Echegoyen, L. *J. Am. Chem. Soc.* **1992**, *114*, 3978. (c) Ohsawa, Y.; Saji, T. *J. Chem. Soc., Chem. Commun.* **1992**, 781. (d) Zhou, F.; Jehoulet, C.; Bard, A. J. *J. Am. Chem. Soc.* **1992**, *114*, 11004.

(2) For reviews on electroactive organofullerenes see: (a) Echegoyen, L.; Echegoyen, L. E. *Acc. Chem. Res.* **1998**, *31*, 593. (b) Martin, N.; Sanchez, L.; Illescas, B.; Perez, I. *Chem. Rev.* **1998**, *98*, 2527.

(3) For reviews on organometallic complexes of fullerenes see: (a) Stephens, A. H. H.; Green, M. L. H. *Adv. Inorg. Chem.* **1997**, *44*, 1. (b) Balch, A. L.; Olmstead, M. M. *Chem. Rev.* **1998**, *98*, 2123.

(4) (a) Koefod, R. S.; Xu, C.; Lu, W.; Shapley, J. R.; Hill, M. G.; Mann, K. R. *J. Phys. Chem.* **1992**, *96*, 2928. (b) Lerke, S. A.; Parkinson, B. A.; Evans, D. H.; Fagan, P. J. *J. Am. Chem. Soc.* **1992**, *114*, 7807. (c) Park, J. T.; Cho, J.-J.; Song, H.; Jun, C.-S.; Son, Y.; Kwak, J. *Inorg. Chem.* **1997**, *36*, 2698. (d) Chernega, A. N.; Green, M. L. H.; Haggitt, J.; Stephens, A. H. H. *J. Chem. Soc., Dalton Trans.* **1998**, 755.

(5) (a) Shapley, J. R.; Du, Y.; Hsu, H.-F.; Way, J. J. In *Recent Advances in the Chemistry and Physics of Fullerenes and Related Materials*; Kadish, K. M., Ruoff, R. S., Eds.; Electrochemical Society Proceedings: Pennington, NJ, 1994; Vol. 94-24, p 1255. (b) Magdesieva, T. V.; Bashilov, V. V.; Gorel'sky, S. I.; Sokolov, V. I.; Butin, K. P. *Russ. Chem. Bull.* **1994**, *43*, 2034.

(6) (a) Hsu, H.-F.; Shapley, J. R. *J. Am. Chem. Soc.* **1996**, *118*, 9192. (b) Lee, K.; Hsu, H.-F.; Shapley, J. R. *Organometallics* **1997**, *16*, 3876. (c) Lee, K.; Shapley, J. R. *Organometallics* **1998**, *17*, 3020.

(7) (a) Song, H.; Lee, K.; Park, J. T.; Choi, M.-G. *Organometallics* **1998**, *17*, 4477. (b) Song, H.; Lee, Y.; Choi, Z.-H.; Lee, K.; Park, J. T.; Kwak, J.; Choi, M.-G. *Organometallics* **2001**, *20*, 3139.

(8) Lee, K.; Song, H.; Kim, B.; Park, J. T.; Park, S.; Choi, M.-G. *J. Am. Chem. Soc.* **2002**, *124*, 2872.

(9) Johnson, B. F. G.; Lewis, J.; Nelson, W. J. H.; Nicholls, J. N.; Puga, J.; Raithby, P. R.; Rosales, M. J.; Schroder, M.; Vargas, M. D. *J. Chem. Soc., Dalton Trans.* **1983**, 2447.

(10) Drake, S. R. *Polyhedron* **1990**, *9*, 455.

(11) Clark, R. J. H.; Dyson, P. J.; Humphrey, D. G.; Johnson, B. F. G. *Polyhedron* **1998**, *17*, 2985.

(12) Shephard, D. S.; Johnson, B. F. G.; Harrison, A.; Parsons, S.; Smidt, S. P.; Yellowlees, L. J.; Reed, D. *J. Organomet. Chem.* **1998**, *563*, 113.

(13) Adams, R. D.; Wu, W. *J. Cluster Sci.* **1991**, *2*, 271.

(14) Nashner, M. S.; Frenkel, A. I.; Adler, D. L.; Shapley, J. R.; Nuzzo, R. G. *J. Am. Chem. Soc.* **1997**, *119*, 7760.

(15) Nashner, M. S.; Frenkel, A. I.; Somerville, D.; Hills, C. W.; Shapley, J. R.; Nuzzo, R. G. *J. Am. Chem. Soc.* **1998**, *120*, 8093.

(16) Hills, C. W.; Nashner, M. S.; Frenkel, A. I.; Shapley, J. R.; Nuzzo, R. G. *Langmuir* **1999**, *15*, 690.

10.1021/om020553d CCC: $22.00
Publication on Web 08/20/2002

rivative $PtRu_5C(CO)_{14}(COD)$[13] has been used to deposit bimetallic nanoparticles on carbon nanotubes.[17] Complex **3** can be viewed as a molecular model for the first step in these interactions of the cluster with the carbon supports. This paper presents our electrochemical and chemical studies of C_{60} complexes **1**−**3** together with some related clusters.

Experimental Section

Ortho-dichlorobenzene, tetrabutylammonium tetrafluoroborate, and cobaltocene were used as received from Aldrich Chemical Co. C_{60} was purchased from Southern Chemical Group and was used as received. The compounds $Ru_5C(CO)_{11}(PPh_3)C_{60}$,[6c] $Ru_5C(CO)_{10}(dppf)C_{60}$,[6c] $PtRu_5C(CO)_{11}(dppe)C_{60}$,[6c] $Ru_5C(CO)_{15}$,[18] $Ru_5C(CO)_{14}(PPh_3)$,[18] $Ru_5C(CO)_{13}(dppf)$,[6c] $PtRu_5C(CO)_{16}$,[13] and $PtRu_5C(CO)_{14}(dppe)$[6c] were prepared by literature methods. IR spectra of all compounds were obtained in solutions of 0.1 M $[(n\text{-}Bu)_4N][BF_4]$ (TBAB) in 1,2-dichlorobenzene (ODCB). IR spectra were recorded on Perkin-Elmer 1710 and 1600 FT-IR spectrometers.

The concentrations of the compounds under study in the electrochemical solutions ranged from 0.2 to 0.8 mM. The supporting electrolyte/solvent system was TBAB in ODCB, with the TBAB concentration 0.1 M unless otherwise noted. Electrochemical experiments were performed with a BAS 100B/W electrochemical analyzer, using a conventional three-electrode cell. The working electrode was glassy carbon (diameter = 3 mm) and was polished with alumina, followed by sonication in deionized water, prior to use. A Ag/AgCl reference electrode and a platinum wire auxiliary electrode completed the cell. Rotating disk electrode voltammograms were obtained using a BAS RDE 1 accessory. All solutions were purged with nitrogen prior to, and blanketed with nitrogen during, the electrochemical experiments. All experiments were conducted at ambient temperature. Unless otherwise stated, peak potentials were obtained from cyclic voltammograms at a scan rate of 100 mV/s and are referenced versus an internal ferrocene standard.

Simulations of cyclic voltammograms were conducted using the DigiSim 2.1 software package (Bioanalytical Systems).[19] The simulations were compared to experimental data collected on a solution of 0.75 mM $Ru_5C(CO)_{10}(dppf)(C_{60})$ (**2**) in 0.4 M TBAB/ODCB. The switching potential was set between the second and third reductions of **2**. The diffusion coefficient of **2** was determined to be 1.6×10^{-6} cm^2/s by fitting simulated data to a scan in which the potential was reversed after the first reduction peak. The diffusion coefficients of the species formed during the reduction and subsequent oxidation processes were also set to this value in the input parameters of the simulation. The transfer coefficient α was set at 0.5 for each electrode reaction. Uncompensated resistance (R_u) and double-layer capacitance (C_{dl}) were incorporated into the simulations, using the values $R_u = 2700\ \Omega$ and $C_{dl} = 1.3\ \mu$F. The solution resistance and RC time constant of the electrochemical solution were determined experimentally by running an "*iR* compensation test" on the BAS 100B/W electrochemical analyzer. The values used for the heterogeneous rate constants were obtained with the simulation software by running a fitting routine while keeping the other parameters constant. After fitting, the heterogeneous rate constants ranged from 1.5×10^{-4} to 6.0×10^{-3} cm/s. The experimental data were collected at several different scan rates ranging from 100 to 600 mV/s. Simulations were run at each of the different scan rates and compared to the corresponding experimental data.

Table 1. Electrochemical Data for {Ru_5C} and {Ru_5C-C_{60}} Complexes[a]

compound	E_{pc1}	E_{pc2}	E_{pc3}	E_{pc4}	E_{pa}
C_{60}[b]	−1.19	−1.59	−2.05	−2.54	
$Ru_5C(CO)_{11}(PPh_3)C_{60}$ (**1**)	−1.16	−1.56	−1.93	−2.53	−0.52
$Ru_5C(CO)_{10}(dppf)C_{60}$[c] (**2**)	−1.20	−1.47	−1.58	−1.97	−0.69
$PtRu_5C(CO)_{11}(dppe)C_{60}$ (**3**)	−1.19	−1.55	−1.92	−2.49	−0.70
$Ru_5C(CO)_{15}$[d] (**4**)	−1.29				−0.39
$Ru_5C(CO)_{14}(PPh_3)$ (**5**)	−1.47				−0.56
$Ru_5C(CO)_{13}(dppf)$ (**6**)	−1.71				−0.85
$PtRu_5C(CO)_{16}$[e] (**7**)	−1.18				−0.24
$PtRu_5C(CO)_{14}(dppe)$ (**8**)	−1.55				−0.58

[a] All potentials are in V vs ferrocene. The solvent/electrolyte system is 0.1 M TBAB/ODCB. Scan rate = 100 mV/s. The typical $E_{1/2}$ of Fc^+/Fc = +0.60 V vs Ag/AgCl, with ΔE_p = ca. 0.2 V. Note: $E_{1/2}$ of cobaltocene = −1.34 V. [b] The corresponding $E_{1/2}$ values for C_{60} were at −1.08, −1.48, −1.94, and −2.45 V. [c] Additional ill-defined reduction peak seen at ca. −2.5 V. [d] Smaller reduction peak also seen at ca. −2.0 V. [e] Additional reduction peak seen at −2.51 V and corresponding oxidation peak at −1.65 V.

Results

Redox Properties of Clusters 4−8. The redox properties of several clusters incorporating {Ru_5C} units have been characterized in order to understand the basic behavior of the metal core prior to C_{60} substitution. Cyclic voltammograms of compounds $Ru_5C(CO)_{15}$ (**4**), $Ru_5C(CO)_{14}(PPh_3)$ (**5**), $Ru_5C(CO)_{13}(\mu\text{-}\eta^1,\eta^1\text{-dppf})$ (**6**), $PtRu_5C(CO)_{16}$ (**7**), and $PtRu_5C(CO)_{14}(dppe)$ (**8**) all exhibit irreversible reduction waves. The cathodic peak potentials of these clusters, along with the anodic peak potentials of the corresponding reduced species, are recorded in Table 1. Cluster **4** has been reported to reduce by an irreversible two-electron process, with concomitant loss of CO, to form the dianion $[Ru_5C(CO)_{14}]^{2-}$ (**4r**$^{2-}$).[9] The oxidation peak potential of **4r**$^{2-}$ that we observe in ODCB (E_{pa} = −0.39 V vs Fc^+/Fc or +0.21 V vs Ag/AgCl) is similar to the previously reported peak potential for oxidation of **4r**$^{2-}$ in CH_2Cl_2 (E_{pa} = +0.15 V vs Ag/AgCl),[9,10] and the combination of evidence (vide infra) suggests that analogous dianions are formed in each case for **5**−**8**.

Substitution of two CO ligands by dppf on going from **4** to **6** causes the cathodic peak potential to shift by −0.42 V. When one CO ligand of **4** is replaced by PPh_3 to form **5**, the cathodic peak potential is shifted by −0.18 V. Thus, PPh_3 substitution has about half of the effect on the reduction potential of the Ru_5C core as substitution by the diphosphine ligand dppf. This potential is shifted by −0.37 V from **7** to **8** due to the substitution of dppe. This negative shift (ca. 0.2 V per P ligand) is similar to that seen in previous studies involving metal core reduction.[20]

There is also a negative shift in potential upon phosphine substitution for the oxidation of the dianionic species. The shift is −0.17 V from **4r**$^{2-}$ to **5r**$^{2-}$ for PPh_3 substitution, −0.46 V from **4r**$^{2-}$ to **6r**$^{2-}$ for dppf substitution, and −0.34 V from **7r**$^{2-}$ to **8r**$^{2-}$ for dppe substitution. Again, shifts of this magnitude have been seen for oxidation of substituted anionic clusters.[20]

There is a relatively constant difference of ca. +0.9 V in E_{pc} for reduction of the neutral compounds **4**−**8** and E_{pa} for oxidation of the corresponding dianions. Data previously reported[12] for $Ru_6C(CO)_{17}$ and for $Ru_6C(CO)_{15}(\mu\text{-dppm})$ also follow this trend.

(17) Hermans, S.; Sloan, J.; Shephard, D. S.; Johnson, B. F. G.; Green, M. L. H. *Chem. Commun.* **2002**, 276.
(18) Johnson, B. F. G.; Lewis, J.; Nicholls, J. N.; Puga, J.; Raithby, P. R.; Rosales, M. J.; McPartlin, M.; Clegg, W. *J. Chem. Soc., Dalton Trans.* **1983**, 277.
(19) Rudolph, M.; Reddy, D. P.; Feldberg, S. W. *Anal. Chem.* **1994**, *66*, 589A.
(20) Geiger, W. E.; Connelly, N. G. *Adv. Organomet. Chem.* **1987**, *24*, 87.

Table 2. Infrared Bands of Neutral and Reduced Cluster Compounds[a]

cmpd	ν(CO) (cm^{-1})	cmpd	ν(CO) (cm^{-1})
1	2069(s), 2030(s), 2022(s), 2014(s)	**1r**$^{2-}$	2006(s), 1966(s, sh), 1959(vs), 1941(s), 1907(m, br)
2	2035(w), 2009(s), 1983(w, br)	**2r**$^{2-}$	1993(m, br), 1952(s, br), 1936(m, sh)
3	2044(vs), 2012(vs), 1951(w, br)	**3r**$^{2-}$	1986(s), 1956(vs), 1942(m, sh), 1910(m, br)
4	2067(s), 2034(m), 2015(w)	**4r**$^{2-}$	2032(w), 1975(s, br), 1963(s, sh)
5	2088(w), 2056(s), 2046(m), 2023(s), 2014(m)	**5r**$^{2-}$	2009(w), 1963(s, sh), 1955(vs), 1944(s, sh)
6	2071(m), 2037(m), 2023(s), 2000(m), 1994(m, sh)	**6r**$^{2-}$	1985 (w), 1944(s)
7	2065(s), 2050(vs), 2006(w)	**7r**$^{2-}$	2033(w), 1976(vs, br), 1912(w)
8	2068(w), 2040(s), 2010(m, br)	**8r**$^{2-}$	1991(w), 1950(s), 1941(m, sh), 1916(m)

[a] In 1,2-dichlorobenzene with 0.1 M [(*n*-Bu)$_4$N][BF$_4$].

Chemical reduction of **4**−**8** with cobaltocene provides supporting evidence that these compounds are reduced in a two-electron process (eq 1). Infrared data obtained before and after reduction are reported in Table 2.

$$Ru_5C(CO)_{13}L_2 + 2CoCp_2 \rightarrow [Ru_5C(CO)_{12}L_2]^{2-} + CO + 2[CoCp_2]^+ \quad (1)$$

The addition of approximately 2 equiv of cobaltocene ($E_{1/2} = -1.34$ V vs ferrocene) to a solution of **4** in 0.1 M TBAB/ODCB causes a dramatic change in the infrared spectrum, with a difference of ca. 90 cm^{-1} between the strongest band in the spectrum before and after the addition of cobaltocene. The spectrum of the reduced species **4r**$^{2-}$ closely matches the previously reported IR spectrum of isolated $[N(PPh_3)_2]_2[Ru_5C(CO)_{14}]$.[9] Analogous behavior is exhibited by compound **5** upon addition of cobaltocene, with the intense IR bands shifting to lower energy by ca. 90 cm^{-1} (Figure 1a). The IR spectrum of the reduced species of **5** does not correspond to the IR spectrum of **4r**$^{2-}$, indicating that the reduced species of **5** is $[Ru_5C(CO)_{13}(PPh_3)]^{2-}$ (**5r**$^{2-}$).

In the case of compound **6**, the addition of 2 equiv of cobaltocene is not sufficient to cause a complete reaction, as monitored by IR. This is not surprising, since **6** is reduced at a more negative potential than cobaltocene (see Table 1). However, the addition of approximately 6 equiv of cobaltocene causes the disappearance of bands due to the neutral complex, with the most intense band of the new IR spectrum, attributed to $[Ru_5C(CO)_{12}(dppf)]^{2-}$ (**6r**$^{2-}$), shifted ca. 80 cm^{-1} lower in energy.

The change in the IR spectrum of **7** upon addition of 2 equiv of cobaltocene is similar, with the most intense IR peak shifting to a lower energy by ca. 75 cm^{-1} (Table 2). Also, the changes in the IR spectrum are almost identical to the changes that occur when $Ru_6C(CO)_{17}$ is reduced to $Ru_6C(CO)_{16}^{2-}$.[11] IR spectra taken after the addition of fewer than 2 equiv of cobaltocene indicate the presence of only the neutral compound and the dianion, $PtRu_5C(CO)_{15}^{2-}$ (**7r**$^{2-}$). In the chemical reduction of **8**, approximately 4 equiv of cobaltocene are required to eliminate bands due to the neutral compound from the IR spectrum. The changes in the IR spectrum are consistent with the formation of a dianion, with the intensity of the strongest peak shifting to a value 90 cm^{-1} lower in energy (Figure 1b).

After forming the dianionic species **4r**$^{2-}$ by adding cobaltocene, a CV of the solution yields an oxidation peak at a potential that corresponds to the E_{pa} observed in the direct CV of **4**, confirming that this oxidation peak corresponds to the oxidation of the dianion **4r**$^{2-}$. In the chemically reduced solution, the reduction peak attributed to the two-electron reduction of **4** ($E_{pc} = -1.29$ V) is absent. Analogous behavior is seen in each case for the chemically reduced solutions of clusters **5**−**8**, substantiating the formation of the corresponding dianions.

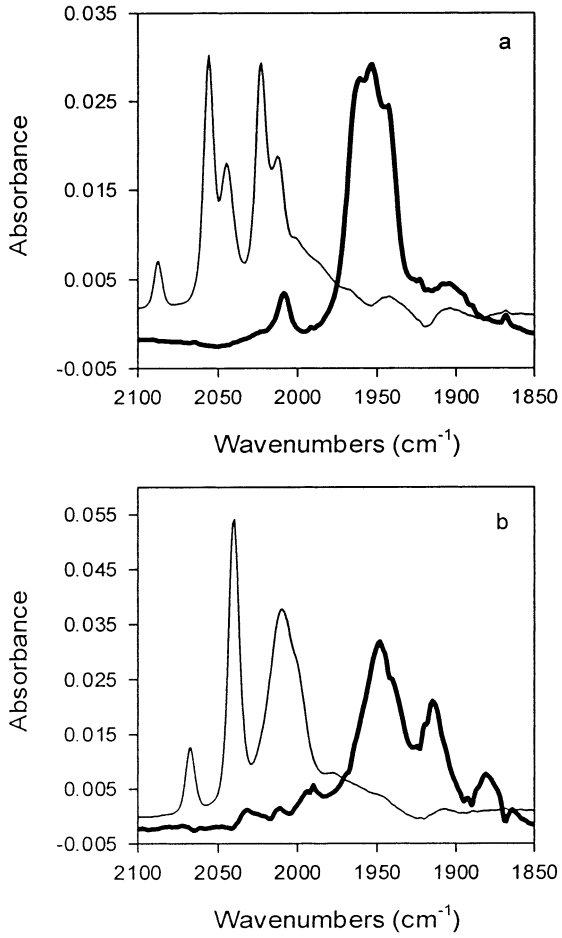

Figure 1. Infrared spectra recorded before (thin line) and after (bold line) reduction by cobaltocene of (a) $Ru_5C(CO)_{14}(PPh_3)$ (**5**) and (b) $PtRu_5C(CO)_{14}$(dppe) (**8**).

Electrochemical and Chemical Reduction of C_{60} Complexes 1 and 3. The CV of compound **1** shows one irreversible two-electron reduction followed by three one-electron quasi-reversible reductions (Figure 2). The third quasi-reversible reduction is near the limit of the solvent window and is not very well-defined in the CV scan; however, this fourth reduction peak is more evident in a differential pulse voltammogram. The cathodic peak currents of the first three reductions have a ratio of approximately 2:1:1; this ratio is confirmed by a potential scan using a rotating disk electrode (Figure 2). If the potential is reversed just after the first reduction wave, the anodic feature seen at −0.52 V is still present (Figure 3). The anodic peak is therefore attributed to the oxidation of **1r**$^{2-}$. The cyclic and RDE

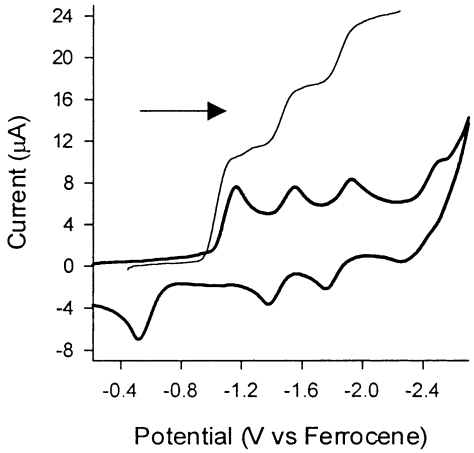

Figure 2. Voltammograms of $Ru_5C(CO)_{11}(PPh_3)C_{60}$ (**1**) in ODCB, 0.1 M $[(n\text{-}Bu)_4N]BF_4$. Bold line: cyclic voltammogram; scan rate = 100 mV/s. Thin line: rotating disk electrode voltammogram; scan rate = 50 mV/s; rotation rate = 400 rpm. Arrow indicates initial scan direction.

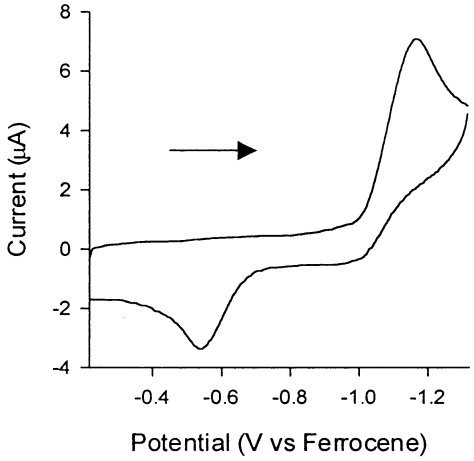

Figure 3. Cyclic voltammogram of $Ru_5C(CO)_{11}(PPh_3)C_{60}$ (**1**) in ODCB, 0.1 M $[(n\text{-}Bu)_4N]BF_4$; potential reversed after first reduction. Scan rate = 100 mV/s. Arrow indicates initial scan direction.

voltammograms of complex **3** display analogous behavior (Figure 4), with the initial two-electron reduction at $E_{pc} = -1.19$ V and the oxidation of $\mathbf{3r}^{2-}$ at -0.70 V.

The IR spectrum taken upon adding 2 equiv of cobaltocene to **1** shows a shift of the ν(CO) bands to lower energies by ca. 60 cm^{-1} (Figure 5a). IR spectra taken after the addition of less than 2 equiv of cobaltocene show peaks from both the neutral complex and those attributed to the dianion. There are no other peaks present, so there is no evidence for a monoanion intermediate. Similar behavior is observed with **3**. The IR band positions of the dianion are shifted by ca. 60 cm^{-1} to lower energy than those of the neutral complex (Figure 5b). An overall two-electron reduction of the metal cluster core, presumably with concomitant carbonyl loss, is indicated for both **1** and **3**.

After chemical reduction by cobaltocene, electrochemical oxidation shows an anodic peak corresponding to oxidation of the dianion at the same position seen in the CVs of neutral **1** or **3**. The cathodic peak for reduction of the neutral compound is only seen after first sweeping through the region in which the dianion is oxidized. Therefore, the overall behavior of **1** and **3**

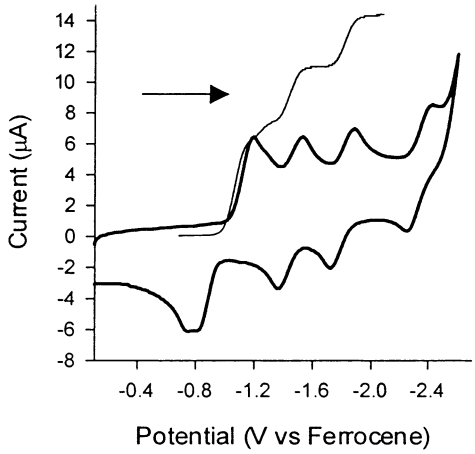

Figure 4. Voltammograms of $PtRu_5C(CO)_{11}(dppe)C_{60}$ (**3**) in ODCB, 0.1 M $[(n\text{-}Bu)_4N]BF_4$. Bold line: cyclic voltammogram; scan rate = 100 mV/s. Thin line: rotating disk electrode voltammogram; scan rate = 20 mV/s; rotation rate = 400 rpm. Arrow indicates initial scan direction.

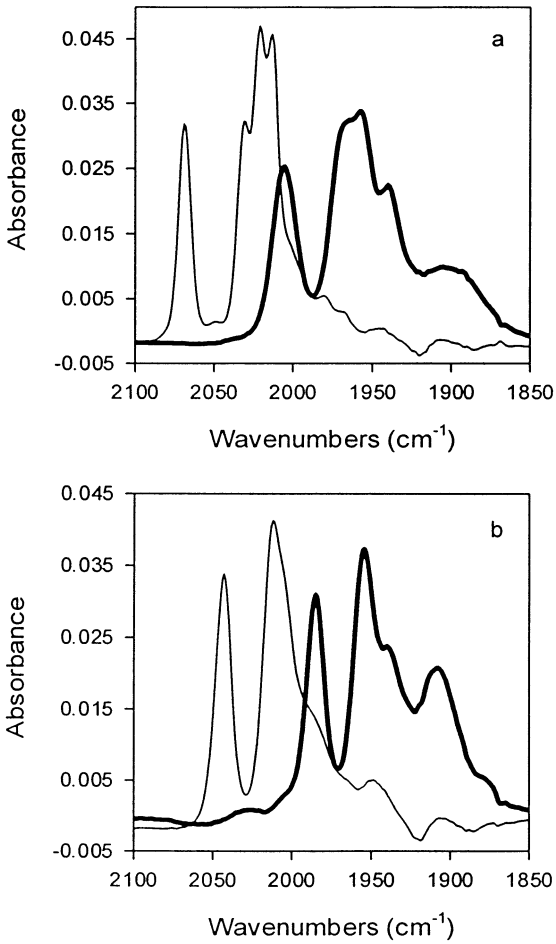

Figure 5. Infrared spectra recorded before (thin line) and after (bold line) reduction by cobaltocene of (a) $Ru_5C(CO)_{11}(PPh_3)C_{60}$ (**1**) and (b) $PtRu_5C(CO)_{11}(dppe)C_{60}$ (**3**).

toward reduction is first the irreversible formation of a metal-core-based dianion followed by stepwise, quasi-reversible reduction of the C_{60} ligand.

Electrochemical and Chemical Reduction of C_{60} Complex 2. The CV of **2** contains four apparently one-electron cathodic peaks, and the 1:1:1:1 current ratio is confirmed by RDE voltammetry (Figure 6). The last two

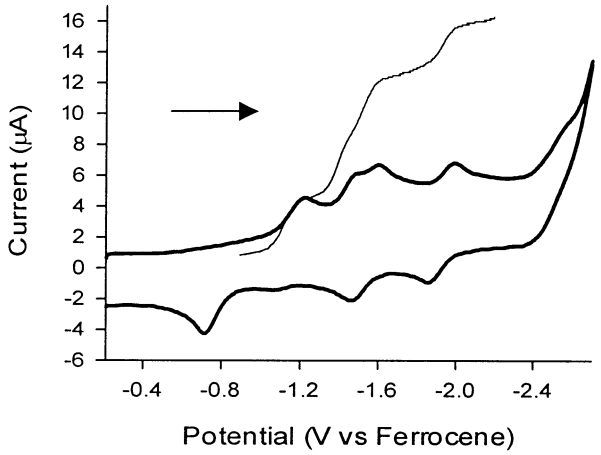

Figure 6. Voltammograms of $Ru_5C(CO)_{10}(dppf)C_{60}$ (**2**) in ODCB, 0.1 M $[(n\text{-}Bu)_4N]BF_4$. Bold line: cyclic voltammogram; scan rate = 100 mV/s. Thin line: rotating disk electrode voltammogram; scan rate = 20 mV/s; rotation rate = 400 rpm. Arrow indicates initial scan direction.

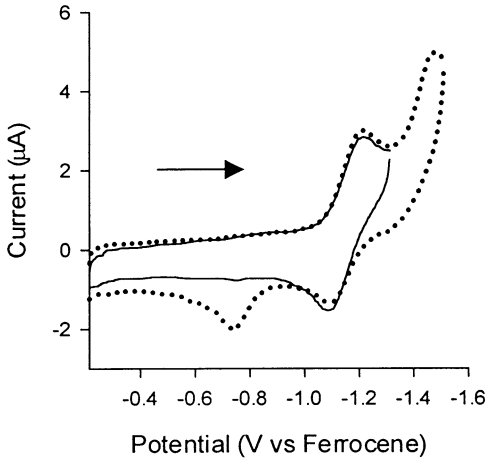

Figure 7. Cyclic voltammograms of $Ru_5C(CO)_{10}(dppf)C_{60}$ (**2**) in ODCB, 0.1 M $[(n\text{-}Bu)_4N]BF_4$. Scan rate = 100 mV/s. Solid line: potential reversed after first reduction peak. Dotted line: potential reversed after second reduction peak. Arrow indicates initial scan direction.

reductions each have an associated oxidation peak and are quasi-reversible processes ($E_{1/2} = -1.52$ and -1.92 V). The first two reductions occur irreversibly ($E_{pc1} = -1.20$ V, $E_{pc2} = -1.47$ V), with only one associated oxidation peak ($E_{pa} = -0.69$ V). However, when the potential scan is reversed at a point between the first and second reduction peaks, the anodic peak at -0.69 V is not present. Instead, there is an anodic peak at -1.06 V, thus making the first reduction a quasi-reversible process ($E_{1/2} = -1.13$ V) (Figure 7). When the potential is reversed past the second reduction peak, both oxidation peaks are present (Figure 7). Upon holding the potential past the second reduction peak prior to scanning in the positive direction, the more negative oxidation peak ($E_{pa} = -1.06$ V), which is due to the oxidation of the monoanion, decreases substantially. After holding the potential constant for 1 min, the monoanion oxidation peak is no longer evident. At the same time, the more positive oxidation peak ($E_{pa} = -0.69$ V) increases. This more positive peak is therefore caused by the oxidation of a species irreversibly formed after the addition of two electrons. The disappearance

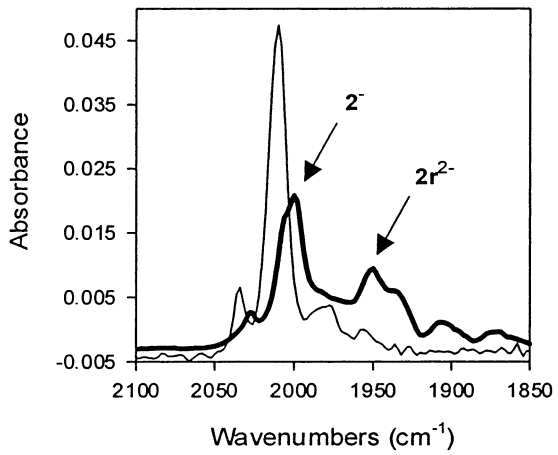

Figure 8. Infrared spectra recorded before (thin line) and after (bold line) the addition of 1 equiv of cobaltocene to a solution (ODCB, 0.1 M $[(n\text{-}Bu)_4N]BF_4$) of $Ru_5C(CO)_{10}(dppf)C_{60}$ (**2**). The principal band at 2000 cm^{-1} is attributed to a monoanionic species ($\mathbf{2}^-$), while the band at 1952 cm^{-1} is attributed to a dianionic species ($\mathbf{2r}^{2-}$). The latter increases with 2 or more equiv of cobaltocene.

of the C_{60} ligand-based oxidation peak in combination with the growth of the cluster-core-based oxidation peak is evidence for the occurrence of an electron transfer from C_{60} to the metal core.

The changes in the IR spectrum accompanying the reduction of **2** by cobaltocene support the CV results. Adding ca. 6 equiv of cobaltocene causes a shift in the IR spectrum consistent with the formation of a cluster-core-based dianion, $\mathbf{2r}^{2-}$, with the most intense peak shifting to a lower energy by ca. 60 cm^{-1}. However, after only 1 equiv of cobaltocene is added, a more modest change in the IR spectrum is seen (Figure 8). Besides the bands due to **2** and $\mathbf{2r}^{2-}$, there are two other bands present that are shifted to lower energies by ca. 8 cm^{-1}. This slight shift is consistent with the shift expected from the formation of a C_{60}-based monoanion,[4a] in this case $[Ru_5C(CO)_{10}(dppf)](C_{60}^-)$ ($\mathbf{2}^-$).

The CV scans of the solution following the addition of 1 equiv of cobaltocene also indicate the presence of the neutral compound, the C_{60}-based monoanion, and the cluster-core-based dianion. A reduction peak consistent with the first reduction of **2** is still present. Also, scanning positively from -1.2 V, when very little cathodic current is seen initially, peaks consistent with both the -0.69 and -1.06 V oxidations are observed. This indicates the presence of both $\mathbf{2}^-$ and $\mathbf{2r}^{2-}$ in solution. When the amount of cobaltocene is increased, the oxidation peak at -1.06 V associated with the oxidation of $\mathbf{2}^-$ disappears. A reduction peak at the same potential as the initial one-electron reduction of **2** is then observed only after generating anodic current in the region of the oxidation peak of $\mathbf{2r}^{2-}$ at $E_{pa} = -0.69$ V.

Simulations of cyclic voltammograms reversed between the second and third reductions were performed. The simulation mechanism also contained equations for the two-electron oxidation of $\mathbf{2r}^{2-}$. Simulations incorporating a one-electron oxidation of $\mathbf{2r}^{2-}$ instead of a two-electron oxidation did not fit the experimental data as well. Simulations were compared to experimental data obtained at scan rates ranging from 100 to 600 mV/s. Over this range in scan rates, the experimentally

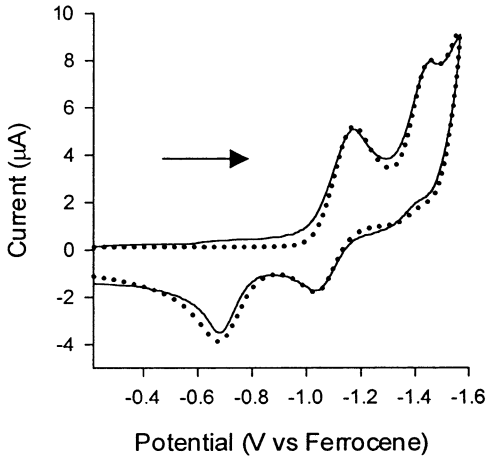

Figure 9. Cyclic voltammogram of $Ru_5C(CO)_{10}(dppf)C_{60}$ (**2**) in ODCB, 0.4 M $[(n\text{-}Bu)_4N]BF_4$, with the potential reversed after second reduction peak. Scan rate = 100 mV/s. Solid line: experimental data. Dotted line: simulation. Arrow indicates initial scan direction.

determined ratio of i_{pa1}/i_{pa2} varies from 0.75 to 1.12. The anodic peak current i_{pa1} is due to the oxidation of $[Ru_5C(CO)_{10}(dppf)](C_{60}^-)$ ($E_{pa1} = -1.06$ V), which occurs prior to the chemical step in the mechanism, and i_{pa2} is the peak current due to the oxidation of $[Ru_5C(CO)_9(dppf)^{2-}](C_{60})$ ($E_{pa2} = -0.69$ V), which follows the chemical step. When the rate constant for the chemical step is set at 10 s^{-1} in the simulation parameters, a good fit to experimental data is obtained throughout the range of scan rates studied. However, the fit is not particularly sensitive to assumed larger values for the rate parameter, so 10 s^{-1} must be viewed as a lower bound. Figure 9 shows experimental and simulated data obtained at a scan rate of 100 mV/s.

Discussion

The behavior observed for compound **2** presents the opportunity to form a coherent view of all three $\{Ru_5C-C_{60}\}$ complexes. The stepwise reduction of **2** appears to involve the steps shown in eqs 2−6.

$$Ru_5C(CO)_{10}(dppf)(C_{60}) + e^- \rightarrow [Ru_5C(CO)_{10}(dppf)](C_{60}^-) \quad (2)$$

$$[Ru_5C(CO)_{10}(dppf)](C_{60}^-) + e^- \rightarrow [Ru_5C(CO)_{10}(dppf)^-](C_{60}^-) \quad (3)$$

$$[Ru_5C(CO)_{10}(dppf)^-](C_{60}^-) \rightarrow [Ru_5C(CO)_9(dppf)^{2-}](C_{60}) + CO \quad (4)$$

$$[Ru_5C(CO)_9(dppf)^{2-}](C_{60}) + e^- \rightarrow [Ru_5C(CO)_9(dppf)^{2-}](C_{60}^-) \quad (5)$$

$$[Ru_5C(CO)_9(dppf)^{2-}](C_{60}^-) + e^- \rightarrow [Ru_5C(CO)_9(dppf)^{2-}](C_{60}^{2-}) \quad (6)$$

The first electron added to **2** clearly resides on the C_{60} ligand (eq 2). Addition of a second electron forces an irreversible loss of carbon monoxide with formation of a reduced metal core (eqs 3, 4). It is probable that the second electron is delivered directly to the metal cluster core (eq 3) and that transfer of the first electron from C_{60} to the cluster core triggers CO loss (eq 4). The CV simulations suggest that the rate of the overall reaction shown in eq 4 is ≥ 10 s^{-1}, but this irreversible homogeneous step cannot be separated very cleanly from the preceding heterogeneous electron-transfer step.

Replacing the diphosphine ligand set of **2** by the monophosphine/carbonyl ligand set of **1** shifts the initial metal core reduction (analogous to eq 3) sufficiently positive that it overlaps with the initial C_{60} ligand reduction. Thus, only the overall irreversible two-electron reduction with CO loss, corresponding to eqs 2−4, is observed. The same situation occurs with compound **3**, where the diphosphine ligand substitution at the platinum atom has an attenuated effect on the core reduction potential. Subsequent stepwise addition of two electrons to the C_{60} ligand is clear for all three compounds (eqs 5, 6), with addition of a third electron occurring near the solvent limit in a largely irreversible fashion.

Complexation of the C_{60} moiety to the $\{Ru_5C\}$ core has a minimal effect on the potential for initial reduction of the C_{60} ligand but a significant effect on the potential for reduction of the cluster core. Thus, as shown in Table 1, E_{pc1} for C_{60} derivative **1** is 0.31 V more positive than for the parent cluster **5**; the analogous shift for **3** vs **8** is 0.36 V. This positive shift provides an indication of the strongly electronegative character of face-bridging C_{60} as a ligand toward the cluster core compared to the three CO ligands it replaces. The shift in metal core reduction potential for **2** vs **6** is (−1.71 V) − (−1.47 V) = 0.24 V. This value is understandably reduced since the C_{60} ligand already has an electron added; the specific value for **2**, however, is also affected by overlap with the subsequent reduction peak.

The peak potentials we observe for oxidation of the reduced $\{Ru_5C\}$ cores in the dianions are not strongly or consistently affected by C_{60} substitution. Thus, $\mathbf{1r}^{2-}$ vs $\mathbf{5r}^{2-}$ at −0.51 vs −0.56 V, respectively; $\mathbf{2r}^{2-}$ vs $\mathbf{6r}^{2-}$ at −0.69 vs −0.85 V, respectively; and $\mathbf{3r}^{2-}$ vs $\mathbf{8r}^{2-}$ at −0.70 vs −0.58 V, respectively. This suggests that the highest energy electrons for these dianions are contained in nonbonding or weakly antibonding MOs associated with the metal cluster unit, probably distributed over π^* levels of the remaining carbonyls.

Electrochemical studies by Park and co-workers on $M_3(\mu_3\text{-}\eta^2,\eta^2,\eta^2\text{-}C_{60})$ complexes have shown no sign of irreversible CO loss from the metal core, with up to four 1*e* reductions occurring in the solvent window.[7] The first two reduction peak potentials are very close to those for free C_{60} (with a slight positive shift), whereas the third and fourth reduction peak potentials are significantly more positive than expected for the C_{60} moiety. Furthermore, phosphine ligand substitution causes negative shifts in the first two potentials of less than 0.1 V but causes a large negative shift in the third potential of 0.3−0.4 V. These results are consistent with theoretical studies of the $Ru_3(CO)_9(\mu_3\text{-}\eta^2,\eta^2,\eta^2\text{-}C_{60})$ complex that indicate the LUMO of the complex is largely comprised of C_{60} atomic orbitals but that the next higher lying MO contains considerable metal orbital charac-

ter.[21] The first reduction potential of $Os_3(CO)_{12}$ has been reported as −1.16 V vs Ag/AgCl[20] which is ca. −1.76 V vs Fc^+/Fc. If substitution of three carbonyls by C_{60} causes a positive shift of ca. 0.20 V in the reduction potential of the Os_3 core, similar to that seen for **2** vs **6** above, then the predicted metal core reduction potential of −1.56 V would be very close to that actually observed for the third reduction of $Os_3(CO)_9(\mu_3\text{-}\eta^2,\eta^2,\eta^2\text{-}C_{60}$ (−1.61 V).[7a] In this case, however, as well as in the Re_3 cluster case, the extra electron added to the metal core can be accommodated without carbonyl ligand loss, possibly due to stronger M−CO bonds for M = Os and Re in comparison with M = Ru.

Acknowledgment. This work was supported by grants from the National Science Foundation, the Office of Naval Research, and the Campus Research Board of the University of Illinois at Urbana−Champaign (UIUC). A.J.B. acknowledges fellowship support from the Department of Chemistry, UIUC, and from the Marshall H. and Nellie Alworth Memorial Fund.

OM020553D

(21) Lynn, M. A.; Lichtenberger, D. L. *J. Cluster Sci.* **2000**, *11*, 169.